

Photoinduced Surface Relief Grating on Amorphous Poly(4-phenylazophenol) Films

Shaoping Bian,[†] Wei Liu,[†] John Williams,[†] Lynne Samuelson,[‡]
Jayant Kumar,[†] and Sukant Tripathy^{*,†}

Departments of Physics and Chemistry, Center for Advanced Materials, University of Massachusetts Lowell, Lowell, Massachusetts 01854, and Materials Science Team, U.S. Army Soldier & Biological Chemical Command Soldier Systems Center, Natick, Massachusetts 01760

Received January 27, 2000. Revised Manuscript Received March 30, 2000

Large-amplitude surface relief gratings on enzymatically synthesized poly(4-phenylazophenol) dye films were holographically induced without postprocessing steps. Recording of the gratings is strongly dependent on the polarization of the writing beams. The phase shift of the topographic grating with respect to the interference pattern was inferred by analyzing a Gaussian laser beam induced surface deformation on the dye film. The mechanism for the surface deformation and grating formation are explained in the framework of the optical field gradient force model.

1. Introduction

Azobenzene chromophore-containing polymer systems have received much attention in the past decade because of their potential uses in various optical applications, such as optical information storage, optical switching, and nonlinear optics.^{1–10} Azobenzene chromophores have been incorporated into the polymer structure in a variety of configurations by a number of different synthetic approaches.¹¹ Optical memory application is one of the areas driving these interests and is based on the large photoinduced optical anisotropy, especially photoinduced birefringence realized in these polymers. Numerous researchers have investigated this phenomenon in various polymer systems, such as guest–host,^{1,2} liquid-crystalline,^{3–5} semicrystalline,⁶ and glassy amorphous polymers among others.^{7–9} Light-induced birefringence in azo compounds is known to be produced by the photoinduced orientation effect of the azobenzene

chromophore. Upon excitation by polarized light, the rodlike azo-dye chromophores undergo repeated trans–cis isomerization accompanied by reorientation until they happen to orient in a plane perpendicular to the polarization direction of the incident light. They remain in that orientation since they cannot be further photoexcited and effects of thermal randomization of the orientation on the azobenzene groups is expected to be slow at temperatures well below the glass transition temperatures (T_g) of the polymer matrix. The photoinduced alignment of azo groups results in a birefringence and absorption dichroism as well. The photoinduced orientation of azo-dye molecules (and therefore the birefringence and absorption dichroism) could be erased by exposure to a circularly polarized or unpolarized light or by simply heating the polymer above its T_g . Therefore, the birefringence resulting from this photoinduced alignment of the azobenzene groups has been used for producing erasable holographic volume gratings.^{1–3,5} The feasibility of recording phase polarization holograms in materials having photoinduced anisotropy was first demonstrated by Kakichashvili¹⁰ and later by Todorov et al.^{1,2} Several groups have reported that gratings with diffraction efficiencies up to 70% can be created. These gratings are formed due to the presence of modulated birefringence in the bulk medium.

Recently it was observed that surface relief gratings (SRG) can be optically produced on azobenzene-functionalized amorphous polymers at temperatures well below the glass transition temperature T_g .^{12,13} Such large-scale polymer mass transport significantly below T_g to create the modulated surface profiles is unusual and has raised important questions about the writing

* To whom all correspondence should be addressed.

[†] University of Massachusetts Lowell.

[‡] U.S. Army Natick.

(1) Todorov, T.; Nikolova, L.; Tomova, N. *Appl. Opt.* **1984**, *23*, 4309.
(2) Todorov, T.; Nikolova, L.; Stoyanova, K.; Tomova, N. *Appl. Opt.* **1985**, *24*, 785.

(3) Eich, M.; Wendorff, J. H.; Reck, B.; Ringsdorf, H. *Makromol. Chem. Rapid Commun.* **1987**, *8*, 59.

(4) Eich, M.; Wendorff, J. H. *J. Opt. Soc. Am. B* **1990**, *7*, 1428.

(5) Wiesner, U.; Reynolds, N.; Boeffel, C.; Spiess, H. W. *Makromol. Chem. Rapid Commun.* **1991**, *12*, 457.

(6) Shi, Y.; Steier, W. H.; Yu, L.; Chen, M.; Dalton, L. R. *Appl. Phys. Lett.* **1991**, *59*, 2935.

(7) Rochon, P.; Gosselin, J.; Natansohn, A.; Xie, S. *Appl. Phys. Lett.* **1992**, *60*, 4.

(8) Natansohn, A.; Rochon, P.; Gosselin, J.; Xie, S. *Macromolecules* **1992**, *25*, 2268.

(9) Kim, D. Y.; Li, L.; Jeng, R. J.; Kumar, J.; Fiddy, M. A.; Tripathy, S. K. *SPIE Proc.* **1993**, *1853*, 23.

(10) Kakichashvili, S. D. *Kvantovaya Elektron.* **1974**, *Moscow 1*, 1435.

(11) Kumar, G. S. *Azo Functional Polymer: Functional Group Approach in Macromolecular Design*; Technomic Publishing Co. Inc.: Lancaster, Basel, 1993.

(12) Kim, D. Y.; Li, L.; Kumar, J.; Tripathy, S. K. *Appl. Phys. Lett.* **1995**, *66*, 1166.

(13) Rochon, P.; Batalla, E.; Natansohn, A. *Appl. Phys. Lett.* **1995**, *66*, 136.

mechanism and its implication on photophysics of azobenzene polymers. With its one-step writing and erasure feature it remarkably distinguishes a number of other technologies of producing topographic gratings that generally involve post wet (or dry) chemical processing. This phenomenon has been explored in a number of azobenzene polymers systems, such as epoxy based, polyacrylates, polyesters, and liquid-crystalline structures among others.^{14–18} Side-chain as well as main-chain azopolymers have been investigated for SRG formation.¹⁹ SRGs, with diffraction efficiency as high as 30–40% in each of the first-order diffraction mode, have been photofabricated using these azopolymers. The formed topographic gratings are stable when kept below T_g , but can be in many cases erased optically or by heating the sample above T_g . This process could be a very useful means to fabricate various complex diffractive optical elements, e.g. infrared waveplates, grating filters, waveguide couplers, and high efficiency gratings for laser and optical applications.^{20–23}

The understanding of the mechanism responsible for the SRG formation is still evolving. The azobenzene chromophore, which undergoes trans–cis–trans isomerization upon photoexcitation, is found to play a key role in the SRG formation. The exploration and understanding of this phenomenon is of significance from both materials chemistry and practical application points of views. In specific systems the erasure of SRG established the reversibility of SRG formation and exclusively ruled out the possibility of photochemical degradation, cross-linking, photobleaching, and laser ablation.²⁴ Strong polarization dependence of writing and erasure has been observed which indicate a photonic process to be responsible for the writing mechanism.²⁵ Several models have been proposed to account for this laser-induced surface deformation.^{14,17,26–28} Our proposed optical field gradient force model adequately explains the polarization dependence of the SRG formation.²⁸ Preliminary experimental results of Gaussian laser beam induced surface deformation recently reported by Bian et al. provides experimental support for this model.²⁹ High

molecular weight linear side chain azobenzene polymers were used in this experiment.

In this paper, we report on the experimental investigation of the holographically inscribed SRG for the first time on films of the new class of nanoscopic poly-(4-phenylazophenol) shape-retentive molecules reported in the previous paper. The macromolecules are made up of 100% azobenzene chromophores and yet the degree of polymerization is modest. Relief grating with diffraction efficiency of 35% was optically produced on this type of polymer film with relative ease. The surface structure of the exposed polymer film was investigated by using atomic force microscopy (AFM). To investigate and understand the mechanism for SRG formation the Gaussian laser beam induced polymer surface deformation experiment, earlier used for high molecular weight polymers, was extended to this system. The experimental results obtained for this new class of macrodye molecules are also found to fit within the framework of the optical field gradient force model. Simultaneous formation of birefringent and absorption grating takes place during the SRG recording and their potential use as a volume holographic recording medium is also recognized. Photoinduced birefringence and absorption dichroism has been experimentally investigated in these films and has been reported in the previous paper of this series.³⁰

2. Experimental Section

2.1. Sample Preparation. The synthesis and characterization aspects of the poly(4-phenylazophenol) used in the investigation is described in detail in previous paper of this series.³⁰ The azo macromolecule was designed for SRG fabrication with a view to highest possible chromophore content in the molecular structure. The oligomeric macrodye molecules possess an articulated shape retentive structure with trans–cis–trans photoisomerization characteristics described in the previous paper of this series.³⁰ Further, the physical dimension of the macromolecule is expected to be ~2–3 nm on the basis of the degree of polymerization of 15 and connectivity through the phenolic groups at the ortho and meta carbons.³⁰ Little or no intermolecular entanglements are expected in the polymer spin-coated films with an isotropic distribution of the chromophores prior to photoexcitation given this low degree of polymerization and articulated structure.

The differential scanning calorimetry (DSC) measurement shows that the polymer has a T_g around 115 °C. This measurement was carried out in nitrogen atmosphere with a scan rate of 10 °C/min. The samples were cooled at the same rate after the first scan, and the T_g value was taken to be the inflection position on the second scan trace. No other thermal transitions are observed either in the cooling or heating cycles confirming only a glassy state.

Optical quality polymer films with different thickness were prepared by spin coating. Polymer solution in spectroscopic grade dioxane was prepared and filtered through a 0.45 μm membrane. The solution was then spin-coated on to glass slides. The film thickness was controlled to 0.2–5.0 μm by adjusting the solution concentration (0.2–0.8 M) and spin speed (3000–7000 rpm). The spin-coated films were then dried under vacuum for 24 h at 40–50 °C and stored in a desiccator until further studies. The spin-coated polymer films were of excellent optical quality and were isotropic. The optical quality films cannot be prepared from the monomer solutions due to the crystallization. The refractive index of the polymer film at 633 nm wavelength is 1.68 (measured by using an ellip-

(14) Jiang, X. J.; Li, L.; Kumar, J.; Kim, D. Y.; Tripathy, S. K. *Appl. Phys. Lett.* **1996**, *68*, 2618.

(15) Kim, D. Y.; Li, L.; Jiang, X. L.; Shivshankar, V.; Kumar, J.; Tripathy, S. K. *Macromolecules* **1995**, *28*, 8835.

(16) Barrett, C. J.; Natansohn, A. L.; Rochon, P. L. *J. Phys. Chem.* **1996**, *100*, 8836.

(17) Ho, M. S.; Barrett, C.; Paterson, J.; Esteghamatian, M.; Natansohn, A.; Rochon, P. *Macromolecules* **1996**, *29*, 4613.

(18) Holme, N. C. R.; Nikolova, L.; Ramanujam, P. S.; Hvilsted, S. *Appl. Phys. Lett.* **1997**, *70*, 1518.

(19) Lee, T. S.; Kim, D. Y.; Jiang, X. L.; Li, L.; Kumar, J.; Tripathy, S. K. *Macromol. Chem. Phys.* **1997**, *198*, 2270.

(20) Tripathy, S. K.; Kim, D. Y.; Li, L.; Kumar, J. *Chemtech* **1998**, *May*, 34–39.

(21) Kipfer, P.; Collischon, M.; Haidner, H.; Schwider, J. *Opt. Eng.* **1996**, *35*, 726.

(22) Liu, J.; Azzam, R. M. A. *Appl. Opt.* **1996**, *35*, 5557.

(23) Boyd, R. D.; Britten, J. A.; Decker, D. E.; Shore, B. W.; Stuart, B. C.; Perry, M. D.; Li, L. F. *Appl. Opt.* **1995**, *34*, 1697.

(24) Jiang, X. L.; Li, L.; Kumar, J.; Tripathy, S. K. *Appl. Phys. Lett.* **1998**, *72*, 2.

(25) Kim, D. Y.; Lee, T. S.; Wang, X.; Jiang, X. L.; Li, L.; Kumar, J.; Tripathy, S. K. *SPIE Proc.* **1997**, *2998*, 195.

(26) Lefin, P.; Fiorini, C.; Nunzi, J. M. *Opt. Mater.* **1998**, *9*, 323.

(27) Pedersen, T. G.; Johansen, P. M.; Holme, N. C. R.; Ramanujam, P. S.; Hvilsted, S. *Phys. Rev. Lett.* **1998**, *80*, 89.

(28) Kumar, J.; Jiang, X. L.; Li, L.; Tripathy, S. K. *Appl. Phys. Lett.* **1998**, *72*, 2096.

(29) Bian, S.; Li, L.; Kim, D. Y.; Williams, J.; Kumar, J.; Tripathy, S. K. *Appl. Phys. Lett.* **1998**, *73*, 1817.

(30) Liu, W.; Bian, S.; Li, L.; Samuelson, L. A.; Kumar, J.; Tripathy, S. *Chem. Mater.* **2000**, *12*, 1577 (preceding article in this issue).

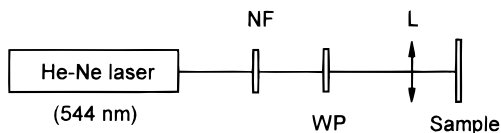


Figure 1. Experimental setup for Gaussian laser beam induced surface deformation.

sometry). The UV–vis absorption spectrum and photoisomerization behavior is reported in the previous paper of this series.³⁰ The thickness of the films were measured by using a Dektak IIA surface profile measuring system.

2.2. Photoinduced SRG Formation. We performed the holographic grating writing experiments using a 4.9 μm thick film sample. The polymer film is exposed to an interference pattern produced by two coherent beams from an argon ion laser at 488 nm.¹² The gratings formed on the polymer sample were monitored by its first-order diffraction in the transmission mode from an unpolarized probe He–Ne laser beam at 633 nm. The probe laser at 633 nm is used since the sample absorption at this wavelength is very small. The intensity of the probe beam is kept low enough so as not to disturb the recording of the gratings. A phase-locked detection technique was used to measure the diffracted light intensity from the grating. Since the polymer film is sufficiently thin the Bragg condition on the incidence angle is not critical in these measurements. The variation on the sample surface that was exposed to the light interference pattern was scanned by AFM 24 h after the recording to ensure that no transient effects are involved. The AFM (Autoprobe CP, Park Scientific Instruments, Sunnyvale, CA) was used in a contact mode for AFM image acquisition. A silicon nitride cantilever with a force constant of 0.26 N/m was used at a scan rate of 1 Hz.

2.3. Gaussian Laser Beam Induced Surface Deformation. To further explore the grating formation mechanism and characterize the phase relationship between the relief grating and the interference pattern, a single laser beam induced surface deformation experiment was carried out. The single Gaussian laser beam experiment has the following advantages: First, its noncontact feature allows a true free surface of polymer to be investigated and avoids any probable restraint and defects caused by other contact methods, e.g. using a transmission mask. Second, the intensity distribution and size of a Gaussian laser beam can be explicitly calculated according to laser propagation theory. Therefore, the spatial relationship between the laser intensity profile and the induced surface deformation can be directly and unambiguously determined by means of microscopic techniques (e.g. AFM). The phase shift of the topographic grating with respect to the interference pattern should be consequently deduced from the Gaussian beam experiments. Insight into the migration of the nanoscopic dye molecules and the nature of the driving force can thus be gained. The experimental setup is schematically shown in Figure 1. A linearly polarized He–Ne laser beam at 544 nm, with a well-defined Gaussian light intensity profile, is focused by a spherical lens. The poly-azophenol sample film is placed at the focal plane of the lens. The intensity of the laser beam is adjusted by inserting different neutral density filters (NF). At the sample surface the radius and central intensity of the laser beam is 3.0 μm and 1.06 W/cm² respectively. The film is exposed for 140 min to the laser beam. The Rayleigh length of the Gaussian laser beam is $\sim 50 \mu\text{m}$, which is much larger than the effective penetration depth of laser beam ($1/\alpha \approx 0.2 \mu\text{m}$, where α is the sample absorption coefficient) at 544 nm. We have recently investigated in detail the nature of surface deformation and possible photothermal and chemical degradation at higher intensity exposure.³¹ None of the typical deleterious features of the effects of high-intensity writing were evident at the intensities used in the present investigation.

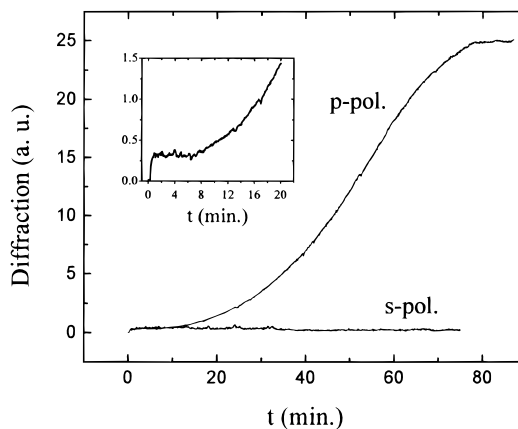


Figure 2. Time evolution of diffraction from the gratings recorded with p-polarization (p-pol) and s-polarization (s-pol) light.

3. Results and Discussion

3.1. Photoinduced SRG Formation. We first performed the grating recording with p-polarized light (the polarizations of the two interfering beams are inside the incidence plane). The curve marked by p-pol in Figure 2 represents a typical time evolution of the probe beam diffraction efficiency of the grating. The intensity of each of the two writing beams used is 100 mW/cm². It was confirmed that similar to the situation of films of higher molecular weight azobenzene polymers, the grating formation is characterized by two processes. The first process saturates in several tens of seconds at the initial stage of the recording as seen in the inset of Figure 2 and gives rise to a maximum diffraction efficiency of about 0.1–0.3%. The latter much slower process, evolves over several tens of minutes and contributes to a large diffraction efficiency. An overall saturable diffraction efficiency of 35% is achieved in our experiments for p-polarization recording. The former (fast grating) is mainly attributed to the bulk refractive index grating formed by the photoinduced birefringence since the absorption grating due to photoinduced dichroism for $\lambda = 632.8 \text{ nm}$ is much smaller than the refractive index grating.³⁰ The effective thickness of the birefringent grating (i.e., the effective penetration depth of recording beams) is $\sim 1/\alpha \approx 0.2 \mu\text{m}$ according to the measured absorption. Therefore, the diffraction efficiency of the bulk birefringent grating is estimated to be 0.2–0.3%, which is consistent with the observed diffraction efficiency in the initial stage of recording. The large diffraction due to the slowly evolved grating can neither be explained by the phase grating formed by the photoinduced birefringence nor by the absorption grating formed by the photoinduced dichroism.

An AFM scan of the exposed sample surface reveals a very regularly patterned SRG as shown by the three-dimensional view in Figure 3 that is responsible for the large diffraction. The micrograph shows that a depth modulation as large as 2000 Å has been inscribed by the light interference pattern at room temperature. The grating spacing measured from AFM is 1.41 μm , which is equal to the period of the interference pattern. The AFM of the sample surface before exposure to laser irradiation reveals a surface roughness of only tens of angstroms. The writing of the SRG has been found to be strongly polarization dependent. The curve marked

(31) Bian, S.; Williams, J.; Kim, D. Y.; Li, L.; W.; Kumar, J.; Tripathy, S. K. *J. Appl. Phys.* **1999**, *86*, 4498.

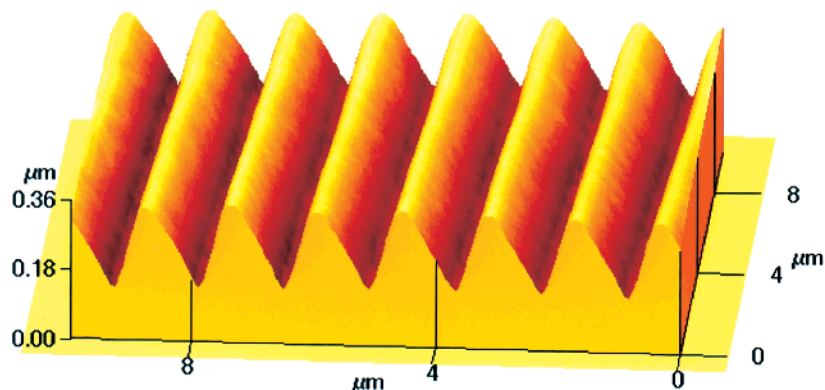


Figure 3. Three-dimensional view of AFM for exposed sample.

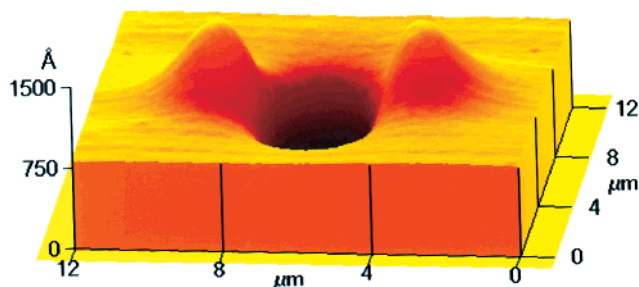


Figure 4. Three-dimensional view of AFM for Gaussian beam exposed sample surface. The laser polarization is along x direction.

by s-pol in Figure 2 represents the time evolution of the diffraction signal of gratings recorded by s-polarization writing (the polarizations of the two writing beams are perpendicular to the incidence plane) with a similar intensity level as in the p-polarization writing (100 mW/cm^2). Only a very small diffraction $\eta = 0.3\text{--}0.4\%$ is detected in this case. The AFM scan of the irradiated film shows a surface relief pattern with depth modulation of less than 80 \AA . SRG with such amplitude modulation can only give a diffraction efficiency of 0.07% . So the diffraction efficiency of $0.3\text{--}0.4\%$ is mainly attributed to the induced bulk birefringent grating. This value is also in good agreement to the theoretically calculated diffraction efficiency for the birefringent grating (see analysis above). We have performed optical erasure experiment with laser irradiation at the same wavelength as writing. Photoerasure behavior is dependent on the polarization of the erasing beam and in certain cases the SRG may not be completely erased.²⁴ The gratings can be completely erased by heating the sample above its glass transition temperature. New topographic gratings can be written again on the refreshed samples.

3.2. Single Gaussian Laser Beam Induced Surface Deformation. Figure 4 shows a three-dimensional view of the AFM of the exposed surface. This AFM displays two significant features. First, the photo-induced surface deformation exhibits strong polarization dependence. The maximum deformation occurs along the direction of laser polarization (the x direction in Figure 4). Second, the surface deformation profile along the polarization is never proportional (positively or negatively) to the laser intensity. Instead, it approximates the second derivative of the laser intensity in the polarization direction (x axis).

3.3. Theory of Laser-Induced Surface Deformation.

The experimental results clearly indicate that the presence of an intensity gradient by itself does not lead to surface deformation unless there is an optical field component present in that direction.^{28,29} These features rule out the possibility that the origin of the laser beam induced surface deformation and the formation of the topographic grating are due to thermal effects and laser ablation. Conformational changes related to isomerization as a basis for these effects is also ruled out as they do not depend on polarization direction of irradiation and should predominantly depend on intensity. This should be especially true for the poly(4-phenylazophenol) where given the crowded backbone of the macromolecule azobenzene chromophores will splay out. The results corroborate a polarization-related surface deformation mechanism. As we asserted in our previous investigation, we believe that a large-scale lateral migration of macromolecules induced by the laser beam has occurred in the single laser beam induced surface deformation process and in the SRG formation. We attribute the force that drives this migration to the optical electric field gradient force. Optically induced gradient forces have been known to affect near-resonant atoms in a vacuum and latex spheres in liquid.^{32–34} A similar mechanism is proposed to be responsible for this laser-induced polymer migration. However, this is the first manifestation of such a process in a solid medium. In the polarizable azopolymer medium, an optical electric field $\mathbf{E}(\mathbf{r}, t)$ induces a medium polarization $\mathbf{P}(\mathbf{r}, t) = \epsilon_0 \chi \mathbf{E}(\mathbf{r}, t)$, where ϵ_0 is the permittivity of vacuum and χ is the medium susceptibility. The time-averaged force density exerted on azo chromophores in a small volume (viewed as a dipole with polarization $\mathbf{P}(\mathbf{r}, t)$) is given by³⁵

$$\mathbf{f} = \langle [\mathbf{P}(\mathbf{r}, t) \cdot \nabla] \mathbf{E}(\mathbf{r}, t) \rangle \quad (1)$$

where $\langle \rangle$ represents the time average. Equation 1 indicates that only in the polarization direction along which there is a component of optical field gradient the azobenzene chromophores experience a force, and the force is vanished when the polarization is orthogonal

(32) Ashkin, A. *Phys. Rev. Lett.* **1970**, *24*, 156.

(33) Smith, P. W.; Ashkin, A.; Tomlinson, W. J. *Opt. Lett.* **1981**, *6*, 284.

(34) Ashkin, A.; Sziezdrim J. M.; Bjorkholm, J. E.; Chu, S. *Opt. Lett.* **1986**, *11*, 288.

(35) Viswanathan, K. N.; Balasubramanian, S.; Li, L.; Kim, D. Y.; Kumar, J.; Tripathy, S. K. *J. Phys. Chem.* **1998**, *102*, 6064.

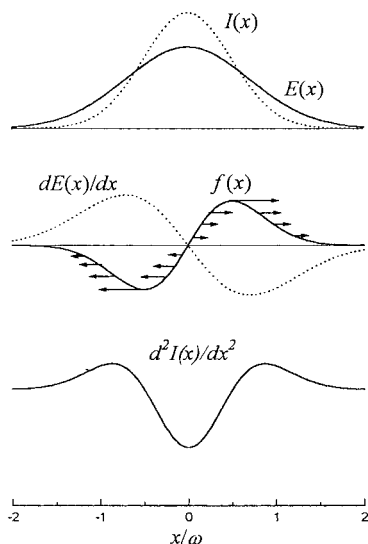


Figure 5. Gradient force distribution.

to the optical field. This feature can be visualized in Figure 4.

In the following analysis, the polarization of the Gaussian beam is assumed to be along the x direction and the sample surface is taken as the x - y plane and the z axis is pointing into the sample medium. Since the laser penetration depth into the polymer film is much smaller ($< 1 \mu\text{m}$) than the Rayleigh length ($\sim 50 \mu\text{m}$) of the Gaussian laser beam used in the experiment, and the sample is placed at the focal plane, the optical field inside the medium can be described by $E(x, y) = E(0) \exp[-(x^2 + y^2)/\omega^2] \exp(-\alpha z/2)$, where $E(0)$ is the optical field at the center of focus. The force density exerted on the azopolymer, according to eq 1, is

$$\mathbf{f}(x, y, z) = \frac{1}{4} \epsilon_0 \chi' \exp(-\alpha z) \frac{\partial I(x, y)}{\partial x} \mathbf{x}_0 \quad (2)$$

where χ' is the real part of the susceptibility of polymer medium. $I_0 = E^2(0)$, $I(x, y)$ is the intensity distribution of the Gaussian beam at the focal plane and \mathbf{x}_0 is the unit vector along the x direction. The experimental results reveal that the macromolecules move out from the light-irradiated region to the nonirradiated region. Therefore, the force direction is away from the center of the Gaussian beam, which implies $\chi' < 0$. The index of refraction of the polymer in the light irradiated region decreases in the direction of polarization.¹

To explicitly indicate the gradient force \mathbf{f} and its relationship with the optical field, Figure 5 depicts the optical intensity $I(x)$, optical field $E(x)$, gradient $dE(x)/dx$, and the gradient force $f(x)$ at $y = z = 0$. The arrows in this figure indicate the force directions. Our earlier investigations have established that laser-induced surface-relief growth on azopolymers is a surface-initiated process rather than a bulk flow phenomenon.^{28,35} The growth of surface relief depends on the movement of an extremely thin surface layer (on the order of 10 nm) at a time. The flow of this mobile layer can be described by a limiting surface velocity field \mathbf{v}_s :

$$\mathbf{v}_s(x, y, z) = \mu \mathbf{f}(x, y, z) \quad (3)$$

where μ is a proportionality factor, which is a function of polymer viscosity and the size and shape of the

polymer chain. This factor incorporates the effects of viscous drag between the mobile layer and the bulk medium. This factor is considered to be independent of the illumination in the current experimental configuration (low intensity regime)³⁶ in the small deformation regime. For an incompressible polymer the surface deformation rate $v_z(x, y, 0)$ can be found from the equation of continuity

$$\nabla \cdot \mathbf{v} = 0$$

$$\frac{\partial v_z}{\partial z} = - \left(\frac{\partial v_x}{\partial x} + \frac{\partial v_y}{\partial y} \right) = - \nabla_s \cdot \mathbf{v}_s \quad (4)$$

$$v_z(x, y, d) - v_z(x, y, 0) = - \int_0^d (\nabla_s \cdot \mathbf{v}_s) dz = - \mu \int_0^d (\nabla_s \cdot \mathbf{f}) dz = - \mu h [\nabla_s \cdot \mathbf{f}]_{z=0} \quad (5)$$

with the boundary condition $v_z(x, y, d) = 0$. Here $\nabla_s = (\partial/\partial x)\mathbf{x}_0 + (\partial/\partial y)\mathbf{y}_0$, \mathbf{y}_0 is the unit vector along the y direction, d ($\ll 1/\alpha$) and h are the total thickness and the effective thickness of the mobile layer, respectively. For a Gaussian beam with linear polarization along x direction $\mathbf{f}(x, y, z)$ (and $\mathbf{v}_s(x, y, z)$) has only x component as shown by eq 2. Therefore, $v_z(x, y, 0)$ and the amplitude of surface deformation in the small amplitude approximation are

$$v_z(x, y, 0) = \frac{1}{4} h \mu \epsilon_0 \chi' \frac{\partial^2 I(x, y)}{\partial x^2}$$

$$S(x, y, t) = \int_0^t v_z(x, y, 0) dt = \frac{1}{4} h \mu \epsilon_0 \chi' \frac{\partial^2 I(x, y)}{\partial x^2} t \quad (6)$$

Equation 6 indicates that the surface deformation profile maps the second derivative of intensity distribution and that the time evolution of diffraction efficiency should exhibit a quadratic time dependence in the regime of small diffraction efficiency. The first result is indeed confirmed in the single beam experiment. The second prediction is confirmed by the measured (p-pol) diffraction efficiency dependence shown in Figure 2. Figure 5 shows also the second derivative of light intensity. It is easy to show that the two maxima occur at $\pm x_m/\omega = \pm \sqrt{3}/4 = \pm 0.866$. Thus, the distance between the two maxima fulfills the expression $\Delta x_m = 1.73\omega$. This value is $5.36 \mu\text{m}$ for our experimental configuration. The experimentally measured result $\Delta x_m = 5.47 \mu\text{m}$ ($= 1.76\omega$) is in close agreement to the calculated result. Figure 6 shows the theoretically calculated surface deformation induced by a linearly polarized Gaussian laser beam using the experimental parameter $\omega = 3.0 \mu\text{m}$. This simulation demonstrates a close similarity to the experimental result.

The experimental results show unambiguously that upon illumination the macrodye molecules move out of the maximum light intensity region in the direction of the polarization vector. From this result we can come directly to the conclusion that the phase-shift of the two-beam interference recorded SRG with respect to the light interference pattern is 180° . This conclusion and

(36) The temperature change is estimated to be less than 10^{-2} K in the current experimental configuration. So the property change of polymer due to the temperature variation is negligible.

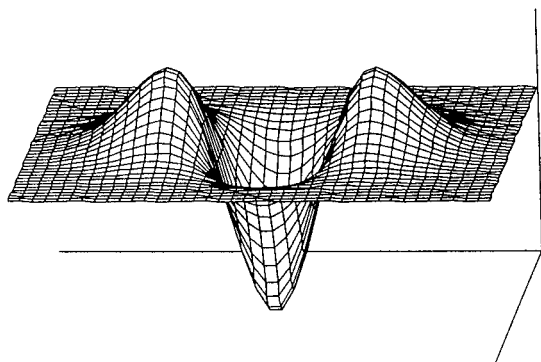


Figure 6. A theoretical simulation using experimental parameter $\omega = 3.0 \mu\text{m}$.

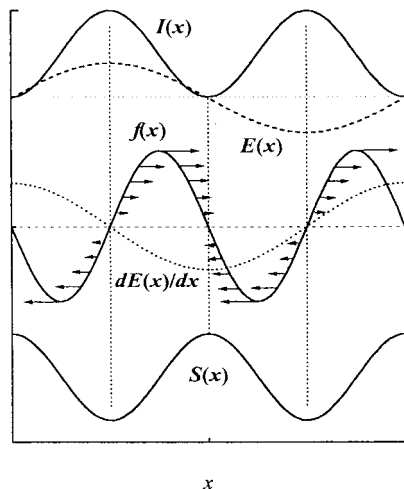


Figure 7. SRG formation and its phase-shift with respect to the interference pattern.

the relief grating formation are analyzed schematically in Figure 7 according to the single beam experimental result and our model. Figure 7 shows respectively the distribution of the sinusoidal light intensity pattern $I(x)$ created by two-beam interference, the corresponding optical field $E(x)$, the optical field gradient $dE(x)/dx$, the optical field gradient force $f(x)$ exerted on the macro-

molecules and the formed SRG profile $S(x)$. At the extreme point of the interference pattern the gradient of optical field changes its sign. Consequently, the optical field gradient force changes its direction. At the position of the maximum intensity the macromolecules are pulled out in the opposite direction, so a dip appears. Inversely, at the position of the minimum the macromolecule molecules were pulled in from two sides and pile up. Therefore, the formed relief grating is π phase-shifted with respect to the interference pattern.

4. Conclusions

In conclusion, we have characterized the formation of the SRG on poly(4-phenylazophenol) films. The oligomeric, articulated, all-azobenzene macrodye molecules form optical quality glassy films. Light-driven surface deformation on these films can be easily carried out as earlier observed for higher molecular weight linear azobenzene polymer glassy films. The efficiency of the topographic grating formation and the photoinduced surface deformation depends on the polarization of the writing laser beam. The experimental results are explained in the framework of the optical field gradient force model. Unusual photoanisotropic behavior and light-induced mass transport appears to be a general feature of macromolecules functionalized with azobenzene chromophores in a variety of ways including the shape-retentive oligomeric macrodye molecules investigated in the present case.

The single beam experiment used in this work is particularly relevant to reveal the photoinduced lateral migration of the dye molecules and to deduce the phase shift of the SRG relative to the interference pattern. The properties observed in this investigation and in the previous paper of this series³⁰ make this class of nanoscopic molecules promising materials for optical data storage and optoelectronics applications.

Acknowledgment. We thank Dr. Lian Li and Dr. Dong-Yu Kim for useful discussions. Financial support from NSF-DMR is acknowledged.

CM000071X